

Deviated well sonic logs, anisotropy and AVA

Scott Leaney, Qeye; Brian Hornby, Hornby Geophysical LLC

Summary

Sonic logs are essential data for seismic reservoir characterization. For example, they are needed for prestack well tie and to construct priors for AVA inversion. The quest for ever more quantitative interpretations means that anisotropy needs to be included in prestack (AVO/AVA) inversion. Sonic logs acquired in deviated wells or in vertical wells drilled through dipping formations are affected by anisotropy, so we investigate the impact of TTI anisotropy on the essential sonic measurements critical for seismic AVA inversion, namely V_p and V_s (and hence acoustic impedance or I_p , and V_p/V_s).

A complicating factor is that sonic tools measure group slowness rather than phase slowness, and this makes the problem nonlinear. We review the theory behind group velocity computation and show that even moderate anisotropy has a significant impact on sonic V_p and V_p/V_s in deviated wells. Thus, corrections are needed if deviated well sonic logs are to be used quantitatively in AVA inversion. We discuss an exact algorithm to correct sonic velocity measurements for the effect of TTI anisotropy given relative dip and show the impact on prestack synthetics and interface AVA.

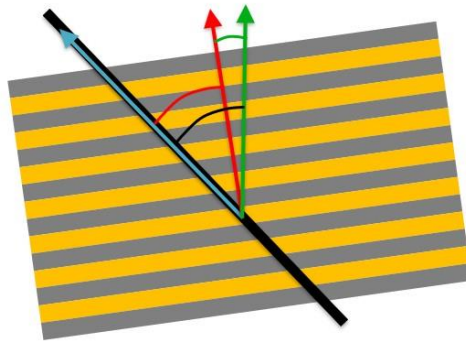
Background

The influence of well deviation on sonic logs has been known for some time. Furre and Brevik (1998) characterized an angle dependency of sonic logs; Hornby et al. (1999) analyzed compressional sonic logs from multiple deviated wells in the context of anisotropy. The question arose as to whether sonic tools were measuring phase or group slowness. Hornby et al. (2003a) investigated the phase versus group question on finite difference synthetic waveforms and concluded that conventional processing was recovering the group slowness in the wellbore direction. Sinha et al. (2006) concluded that phase slowness was being measured on processed synthetics, but as argued by Miller et al. (2012), they evidently considered phase angle as corresponding to well deviation. Walsh et al. (2007) derived anisotropy parameters in a shale using logs of compressional and shear slownesses from vertical and lateral wells but did not specify whether phase or group was being used for inversion. Sayers et al. (2015) used kriged vertical velocities and deviated well sonic velocities to estimate VTI parameters for several Horne River formations but also did not specify whether phase or group velocity was being inverted. Considering work where group slowness or velocity was stated explicitly as being used, Hornby et al. (2003b) derived anisotropy parameters from compressional logs in multiple deviated wells, using an empirical relation for V_s ; Horne et al. (2012) and Miller et al. (2012) estimated VTI parameters for a long section of Haynesville shale using P , S_v and S_h slownesses, where S_v and S_h data were obtained from crossed-dipole processing; Jocker and Hansen (2021a, 2021b) discussed an algorithm which includes cluster analysis wherein sonic logs from multiple deviated wells were used to estimate continuous logs of TI parameters.

Regarding the correction of logged slownesses or velocities to the symmetry axis direction, Hornby et al. (2003b) proposed an algorithm to correct compressional sonic logs acquired in deviated wells for the purpose of improving well tie. Horne et al. (2012) corrected

compressional and shear logs from a deviated lateral well and compared those to logs from a nearby vertical well. These authors did not discuss the correction process nor the application to prestack seismic data. Far and Mekic (2016) discussed an algorithm to estimate and correct monopole P and S logs but used phase velocity.

In this paper we discuss exact and approximate TTI correction algorithms for both Vp and Vs and look at the impact of anisotropy on sonic logs in the context of prestack seismic (AVA) inversion. Figure 1 shows a schematic of the problem. A dipping formation is penetrated by a deviated borehole. The symmetry axis of the formation is at some angle to the wellbore. From the measured sonic slownesses along the borehole we seek to recover Vp and Vs in the direction of the symmetry axis. We also need the vertical velocity for depth-to-time conversion. We assume that logs of anisotropy parameters are available (a separate problem, see Discussion).



- We seek **symmetry axis Vp and Vs** for well tie and AVA and **vertical Vp** for depth-to-time conversion
- We assume TI parameters are known (separate problem)

- Deviated wellbore
- Sonic measurements
 - Group slownesses!
- Symmetry axis velocities
- Vertical P velocity
- Angles:
 - Well deviation, $devi$
 - Formation dip, α
 - Relative dip, $\varphi_d = devi - \alpha$

Figure 1. Schematic of different directional velocities when a deviated borehole penetrates a dipping (TTI) formation. The sonic tool measures group slownesses in the borehole direction, the velocities in the symmetry axis of the formation are desired. The symmetry axis may be inclined with respect to vertical at a relative dip angle to the borehole. The vertical velocity is needed for depth-to-time conversion and may be different from that of the symmetry axis when there is formation dip as in the case of TTI.

Theory

As shown conclusively by Miller et al. (2012), standard sonic processing produces logs of group slowness, not phase slowness. Since we will need to compute group velocity (or slowness) at a group angle equaling relative dip (or well deviation if formation dip is zero), we briefly review the needed theory. Considering the case of general anisotropy with up to twenty-one stiffness moduli, the i -th component of group velocity is given by (Chapman, 2004, (5.3.20))

$$V_i = a_{ijkl} p_k \hat{g}_j \hat{g}_l \quad (1)$$

where a_{ijkl} is the density-normalized 4th order (3x3x3x3) stiffness tensor, \hat{g}_j and \hat{g}_l are components of the normalized polarization vector, \hat{g} , p_k is the k th component of the phase

slowness vector and summation over repeated indices is assumed. To determine \hat{g} , the following eigen (Christoffel) equation (Chapman, 2004, (5.3.26)) must be solved

$$\hat{\mathbf{r}}\hat{g}_I = c_I^2\hat{g}_I \quad (2)$$

for eigenvalues c_I^2 , the squared phase velocities, and eigenvector matrix \hat{g}_I , $I = 1,2,3$, the polarizations for qP , $qS1$, $qS2$ codes. $\hat{\mathbf{r}}$ is the Christoffel matrix given by (Chapman, 2004, (5.3.15)) as

$$\hat{\mathbf{r}} = \hat{p}_j\hat{p}_k\mathbf{a}_{jk} \quad (3)$$

where \mathbf{a}_{jk} are a collection of six 3x3 sub-matrices built up from the density-normalized Voigt moduli (Chapman (4.4.39)). Thus, given the stiffness moduli and having specified a phase direction from angles to get $\hat{p} = (p_1, p_2, p_3)$ for (3), having solved (2) for phase velocities c_I and polarization vectors (\hat{g}_I) and setting $\mathbf{p} = \hat{p}/c_I$ for (1), the above three equations allow the group velocity components to be determined. The group velocity dip and azimuth angles may then be obtained from the group velocity components.

While the above approach for general media is not computationally onerous, many lines of code are needed and simplifications and efficiencies result when media of greater symmetry are considered. For transversely isotropic media, Chapman (2004, section 5.7.1) provides analytical expressions for the horizontal and vertical group velocity components requiring only a few lines of code. This is particularly useful for exact ray tracing in a layered VTI medium (e.g. Leaney, 2014, ch. 3). Mukhopadhyay and Mallick (2011) provide exact expressions for group velocity magnitude and angle in terms of Thomsen (1986) parameters.

It is instructive to look at group and phase velocities for a selected VTI medium with moderate anisotropy. The parameters chosen for the medium are $(V_p, V_s, \text{eps}, \text{del}, \text{gam}) = (4.0, 1.8, 0.25, 0.10, 0.28)$ where velocities are in km/s. This medium possesses a slight triplication in the qSv group velocity surface as can be determined by comparing the positive root of a cubic to an anellipticity parameter (Schoenberg and Helbig, 1997). Thomsen and Dellinger (2003) provide an exact and an approximate triplication condition. Figure 2 shows plots of phase and group velocities versus phase angle and group angle, respectively, for qP , qSv and Sh . To generate these plots, phase angle was incremented at a constant rate. Note that group angle increments differently for the three different codes and that finding the phase angle that gives rise to a given group angle requires either interpolation or a line search inversion for each code. For this moderate amount of anisotropy, the impact on both V_p and V_p/V_s is significant, with the difference between velocity at 0 degrees (symmetry axis) and 40 degrees requiring about a 6% decrease in V_p , a 14% decrease in V_{sv} and an 8% increase in V_p/V_s . It is interesting to note that while the difference from symmetry axis in V_p grows monotonically with angle, the behaviour of V_p/V_s is more complicated due to the behaviour of V_s (middle plot). If the fastest shear is taken as the measured value at every angle (as would likely be the case for legacy monopole logging) and used for the V_p/V_s ratio, then after reaching a maximum difference at just beyond 40 degrees, the difference decreases until the Sh (dashed) leg is met and then remains about constant at 3%. We note that some legacy dipole logs were acquired using only a single dipole source (for logging speed efficiency) which leaves an ambiguity as to which shear slowness was being processed. If crossed-dipole logging and processing is available, then the V_p/V_s ratio using V_s would increase dramatically, becoming a

positive difference (negative correction) beyond about 50 degrees. Such a large difference in sonic shear velocities at high deviation angles is seen in the data of Horne et al (2012) and Miller et al (2012). If the Sh is used then the maximum correction to V_p/V_s is about half that for S_v and retains the same sign with angle. In either case the difference in V_p/V_s relative to the symmetry axis direction becomes significant, noting that the anisotropy used for these plots was *moderate*. Clearly, anisotropy needs to be taken into account if deviated well sonic logs are to be used quantitatively for prestack well tie and as priors in prestack seismic (AVA) inversion.

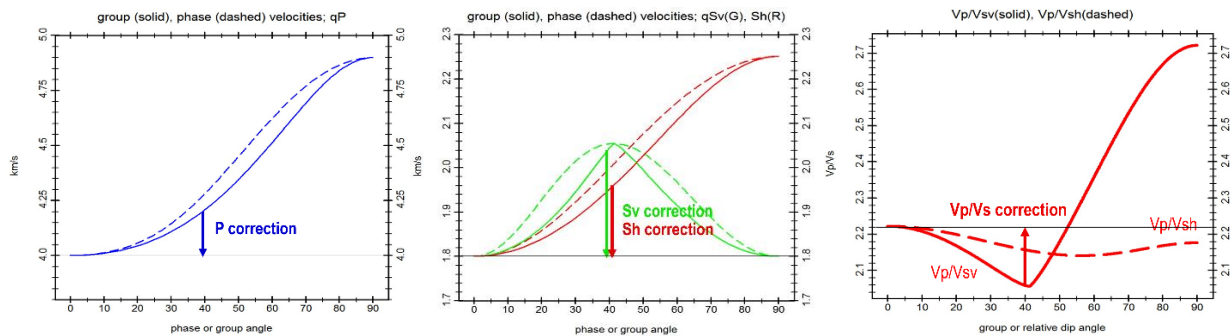


Figure 2. Left: qP phase (dashed) and group (solid) velocities versus angle. Middle: qSv (green) and Sh (red) phase (dashed) and group (solid) velocities versus angle. Right: V_p/V_s versus group angle for $V_s=V_{sv}$ (solid) and $V_s=V_{sh}$ (dashed). Corrections at 40 degrees are indicated.

Since prestack migration (ideally TTI depth migration), produces gathers with offset relative to normal incidence (the symmetry axis direction), the correction of sonic logs measured at some well deviation (or relative dip) to the symmetry axis direction requires some discussion. In what follows, the TI anisotropy parameters are assumed known at each sonic log depth. Ideally these come from a multiwell inversion (Jocker and Hansen, 2021a, 2021b) or from single well sonic anisotropy measurements augmented with *sonic tensor completion* (Leaney and Jocker, 2018), but they may also come from a simple rock physics model where anisotropy is driven by the volume of clay and porosity from petrophysics, for example. Using something plausible (generally positive) will always be better than isotropy (zero). We discuss an exact correction algorithm below but have also used approximate approaches.

The exact algorithm requires two nonlinear inversions. The first is a line search to determine the phase angle that gives rise to the group angle that matches relative dip. For this step we use the secant algorithm. The second inversion is a two-parameter inversion for the symmetry axis velocities, V_{p0} and V_{s0} , that, given anisotropy parameters and relative dip between the wellbore direction and the symmetry axis, reproduce the measured group velocities. For this we use the downhill simplex algorithm “amoeba” (Press et al., 2004). In the next section we show results on field data, illustrating the impact on prestack synthetic seismograms and interface AVA.

Case study

We consider logs from an offshore tertiary sand-shale sequence. The well deviates up to 40 degrees and dip is taken to be zero, so φ_d equals well deviation. Anisotropy was defined using logs of V_{shale} and bulk density. Density was used to calculate porosity to define a compaction trend according to $1 - \phi/\phi_c$, where ϕ_c is critical porosity, taken to be equal to 0.40. Inspired by the work of Bachrach (2012) and Sayers (1994), we define ellipticity, E , and anellipticity, A , parameters (Schoenberg et al., 1996), then transform to Thomsen parameters. We include negative ellipticity and small positive anellipticity in formations with low V_{shale} as these properties were found for stress-sensitive sandstones (Sayers et al., 2024) when vertical stress is assumed to be the maximum principal stress, hence a normal faulting regime. This means that $\delta < \varepsilon < \gamma < 0$ in stress-sensitive sandstones. This was also included in log-scale anisotropic priors by Leaney et al. (2024). Figure 3 shows logs of well deviation, VTI parameters, measured and corrected V_p , measured and corrected V_p/V_s . It is clear that the combination of well deviation and anisotropy results in a reduction in V_p and an increase in V_p/V_s , consistent with the curves shown in figure 2.

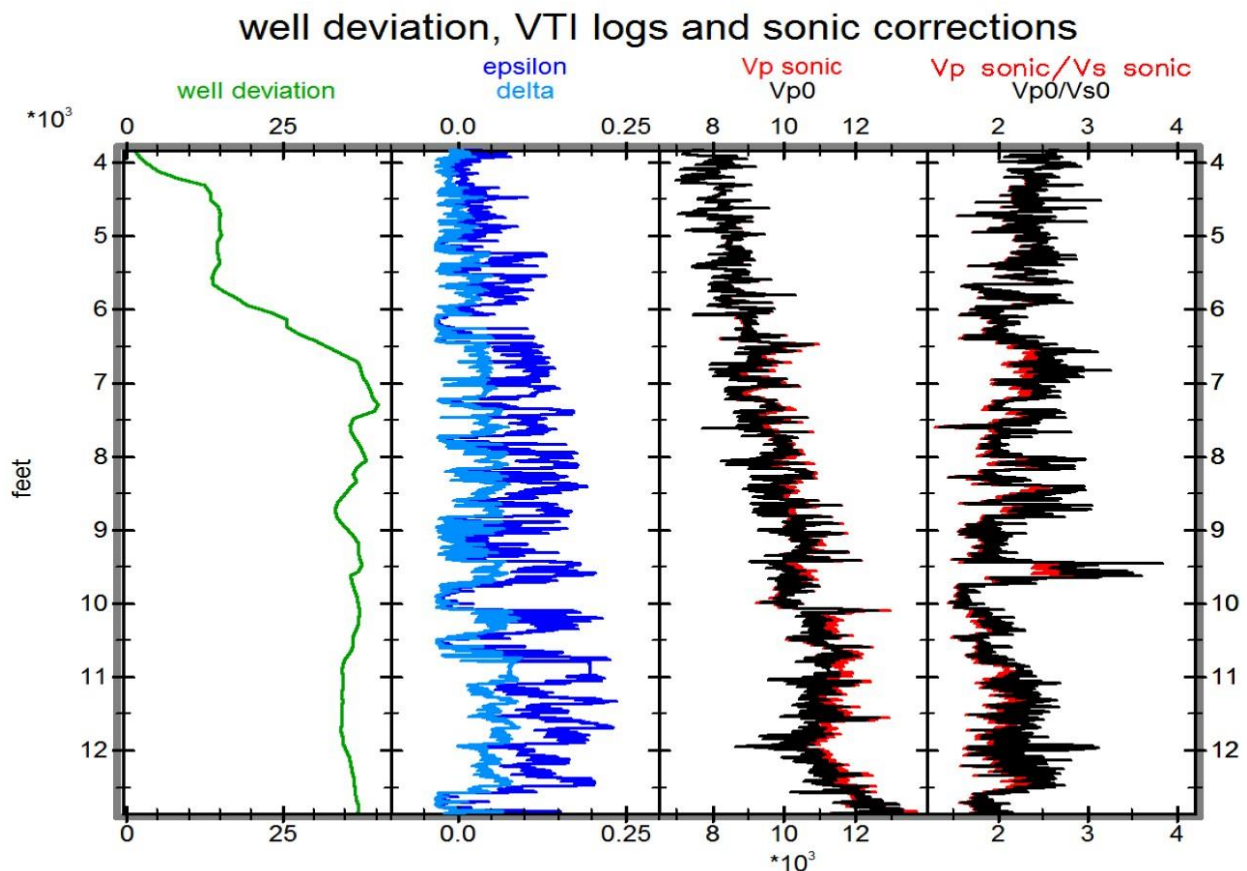


Figure 3. From left to right: well deviation, VTI parameters, V_p , V_p/V_s . Symmetry axis - corrected logs are shown in black.

To show the impact on AVA, two VTI models were built using Backus upscaling and blocking, one for the measured sonic velocities and one for the symmetry axis -corrected velocities.

Exact VTI ray theory synthetics were computed and transformed to angle bands using ray trace phase angles; the vertical velocity models were then used to transform I_p and V_p/V_s models from depth to time. This is shown in Figure 4.

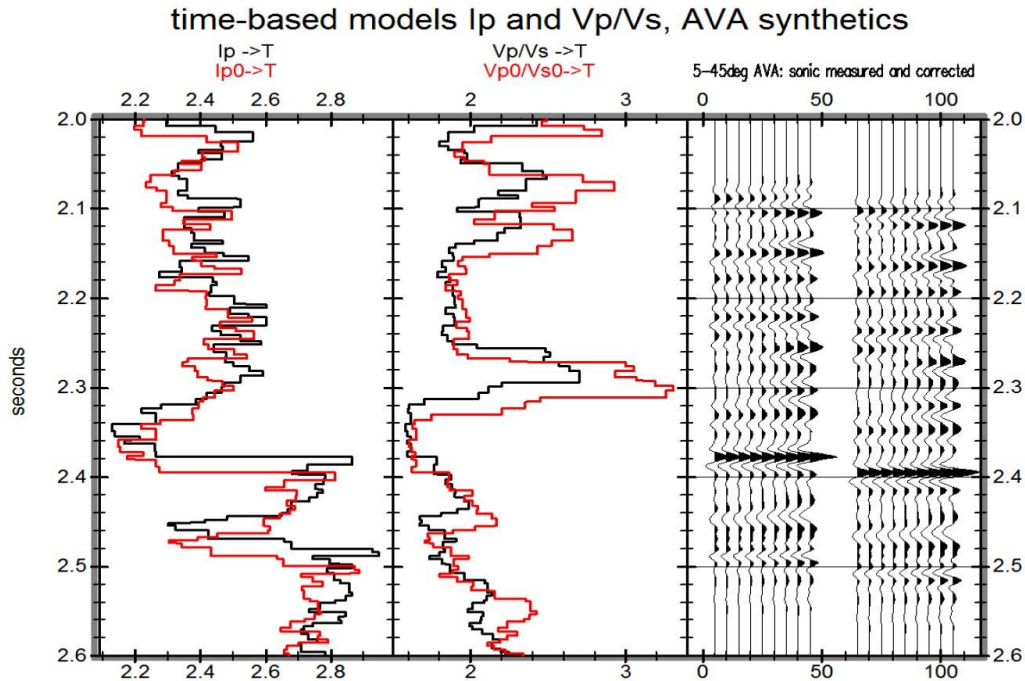


Figure 4. Time-based model properties for I_p and V_p/V_s with symmetry axis -corrected properties in red. 40Hz VTI ray theory AVA synthetics 5-45 degrees are shown on the right, with the corrected-velocity synthetic to the right. The longer time for the corrected-velocity synthetics is due to the lower symmetry axis -corrected velocity, V_{p0} .

Because of the lower V_p in the (vertical) symmetry axis direction, there is a cumulative positive time shift for the symmetry axis model properties and for the AVA synthetics. The differences in AVA responses are present but are difficult to appreciate. To illustrate better, VTI AVA responses are shown in figure 5 for interfaces at top shale (either side of 2.26s) and base reservoir (either side of 2.39s). Note that both the intercept and gradient are impacted and that there is a deceptive effect of making high angle responses nearly overlay.

Discussion

Sonic waveform processing is a non-trivial endeavor, involving array beamforming and dispersion inversion. Crossed-dipole shear processing requires defining a time window and 4C Alford-type rotation. In a deviated well, knowledge of sonde orientation relative to top-of-hole then allows for the labelling of qS_v (vertical plane) and Sh (bedding plane). Other factors include borehole diameter, tool diameter, mud slowness, near-wellbore alteration, permeability effects. Furthermore, a medium with sufficient anellipticity will produce qS_v triplication, leading to a question as to which branch of the qS_v group velocity curve would be found by commercial processing algorithms.

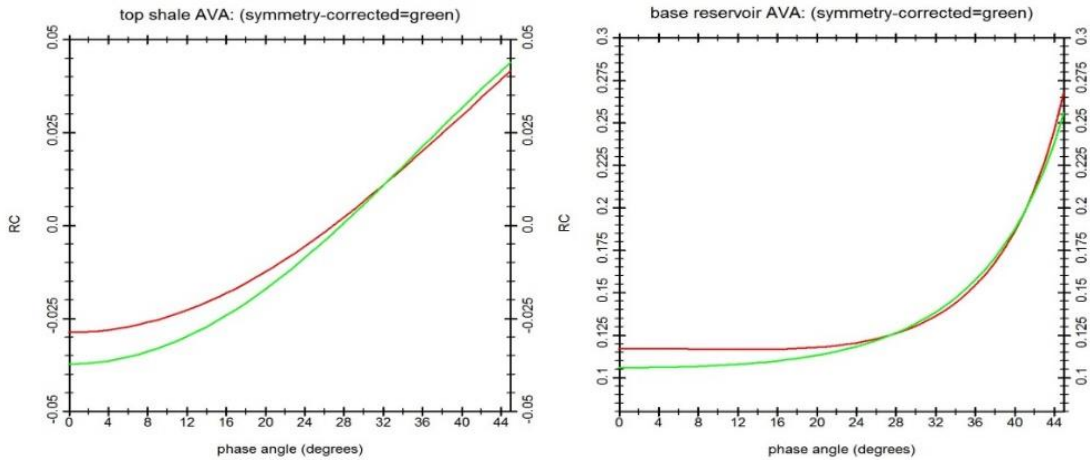


Figure 5. Exact VTI AVA for top shale (left) and base reservoir (right) interfaces. The symmetry axis -corrected responses are shown in green.

Horne et al. (2019) generated FD synthetic dipole sonic waveforms for a triplicating medium and processed using time- and frequency- domain semblance algorithms. They found that separate semblance peaks were difficult to identify, but group slowness (again) fit the data much better than phase slowness. The impact of qSv triplication on commercial sonic shear products requires further investigation. Figure 6 shows phase and group velocities versus angle for a triplicating medium, being parameters for a shale of Ordovician age from North Africa which were determined using a walkaway VSP (Leaney, 2008) using a phase slowness-polarization inversion (Leaney and Hornby, 2007). Looking at the right side of figure 6, observe that between 24° and 63° there are three (group) arrivals with the same (group) angle. We note that if used in an inversion of angle-dependent sonic slowness measurements, fitting multiple qSv arrivals to handle triplication would inject a strong multi-modality into the objective function, necessitating exhaustive global search techniques.

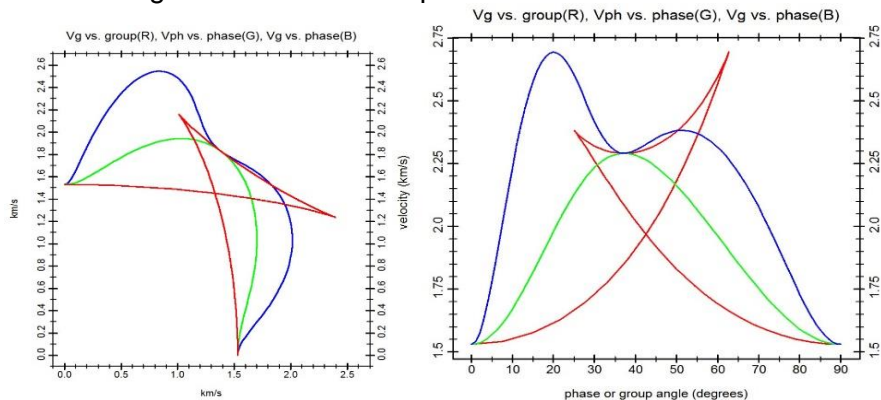


Figure 6. qSv velocities versus angle for a triplicating medium. Phase velocity versus phase angle (green), group velocity versus phase angle (blue), group velocity versus group angle (red). Left: polar plot, right: linear plot. The medium has properties $(V_p, V_s, \epsilon, \delta) = (3.50, 1.53, 0.58, -0.05)$.

Conclusions

In the quest for ever more quantitative interpretations it is important to include anisotropy in AVA inversions. Since sonic logs are essential information for prestack (AVA) seismic inversion, we consider the impact of anisotropy on sonic logs acquired in deviated wells. A complicating factor is that sonic logs measure group slowness (or velocity), not phase slowness. We use an exact algorithm to correct sonic measurements for relative dip so the velocities represent those in the symmetry axis or normal incidence direction. The correction factors are found to be significant, even for moderate anisotropy. The impact on AVA was shown using logs from a tertiary offshore well, making use of anisotropic ray theory synthetics and exact VTI Zoeppritz computations.

References

- Bachrach, R., 2012, Elastic and resistivity anisotropy of shale during compaction and diagenesis: Joint effective medium modeling and field observations: *Geophysics*, **76**, E175-E186.
- Chapman, C.H., 2004, *Fundamentals of seismic wave propagation*, Cambridge University Press.
- Far, M. E., and N. Mekic, 2016, Correction of sonic logs for anisotropy (deviation) effects and handling its nonuniqueness problems: 86th Annual International Meeting, *SEG Expanded Abstracts*, 377–381, doi: 10.1190/segam2016-13863627.1.
- Furre, A.-K., and I. Brevik, 1998, Characterization of angle dependency in sonic logs: *SEG Expanded Abstracts*, 292–295, <http://dx.doi.org/10.1190/1.1820406>.
- Hornby, B. E., J. M. Howie, and D. W. Ince, 1999, Anisotropy correction for deviated well sonic logs: Application to seismic well tie: 69th Annual International Meeting, *SEG Expanded Abstracts*, 112–115, <http://dx.doi.org/10.1190/1.1820700>.
- Hornby, B., J. Howie, and D. Ince, 2003, Anisotropy correction for deviated-well sonic logs: Application to seismic well tie: *Geophysics*, **68**, no. 2, 464–471, <http://dx.doi.org/10.1190/1.1567212>.
- Hornby, B., X. Wang, and K. Dodds, 2003, Do we measure phase or group velocity with dipole sonic tools?: 65th Annual International Conference and Exhibition, *EAGE, Extended Abstracts*, F29.
- Horne, S., Walsh, J. and Miller, D., 2012, Elastic anisotropy in the Haynesville shale from dipole sonic data: *First Break*, **30**, 37–41.
- Horne, S., Coates, R. and Bolshakov, A., 2019, Do dipole sonic logs measure group or phase velocity (revisited): *Geophysics*, **84**, C311–C322.
- Jocker, J. and Hansen, J.-O., 2021a, Bayesian-type TI anisotropy characterization using depth-dependent prior information: *EAGE Proceedings*.
- Jocker, J. and Hansen, J.-O., 2021b, TI anisotropy characterization on basis of sonic data sets from multiple wells: A Norwegian Sea case study: *SEG Expanded Abstracts*.
- Leaney, W.S. and Hornby, B.E., 2007, Depth-dependent anisotropy from walkaway VSP in the Gulf of Mexico: *EAGE Proceedings*.
- Leaney, W.S., 2008, Polar anisotropy from walkaway VSPs: The Leading Edge.
- Leaney, W.S., 2014, *Microseismic source inversion in anisotropic media*: PhD Thesis, UBC.

Leaney S. and Jocker, J., 2018, Sonic tensor completion and applications: *SEG Expanded Abstracts*.

Leaney, S., Sayers, C. and Goodway, B., 2024, Anisotropic priors for probabilistic AVA inversion: *IMAGE*.

Miller, D., S. Horne, and J. Walsh, 2012, Precise inversion of logged slownesses for elastic parameters in a gas shale formation: *Geophysics*, **77**, no. 4, B197–B206, doi: 10.1190/geo2011-0334.1.GPYSA70016-8033

Mukhopadhyay, P.K. and Mallick, S., 2011, An accurate ray-based offset-to-angle transform from normal moveout uncorrected multicomponent data in a transversely isotropic medium with vertical symmetry axis: *Geophysics*, **76**, C41-C51.

Press, W.H., Teukolsky, S.A., Vetterling, W.T. and Flannery, B.P., 2006, *Numerical Recipes*, Cambridge University Press.

Sayers, C.M., 1994, The elastic anisotropy of shales: *Journal of Geophysical Research*, **99**, 767-774.

Sayers, C., den Boer, L., Dasgupta, S. and Goodway, B., 2015, Anisotropy estimate for the Horn River Basin from sonic logs in vertical and deviated wells: *The Leading Edge*, March, 296-306.

Sayers, C.M., Leaney, W.S. and Bratton, T., 2024, Stress-induced anisotropy in Gulf of Mexico sandstones and the prediction of in situ stress: *Geophysical Prospecting*, 1-13, DOI: 10.1111/1365-2478.13497.

Schoenberg, M., and K. Helbig, 1997, Orthorhombic media: Modeling elastic wave behavior in a vertically fractured earth: *Geophysics*, **62**, 1954–1974, <https://doi.org/10.1190/1.1444297>.

Sinha, B. K., E. Simsek, and Q. H. Liu, 2006, Elastic-wave propagation in deviated wells in anisotropic formations: *Geophysics*, **71**, no. 6, D191–D202, doi: 10.1190/1.2358402.GPYSA70016-8033.

Thomsen, L., 1986, Weak elastic anisotropy, *Geophysics*.

Thomsen, L., and J. Dellinger, 2003, On shear-wave triplication in transversely isotropic media: *Journal of Applied Geophysics*, **54**, 289–296, doi: 10.1016/j.jappgeo.2003.08.008.

Walsh, J., B. Sinha, T. Plona, D. Miller, D. Bentley, and M. Ammerman, 2007, Derivation of anisotropy parameters in a shale using borehole sonic data: *SEG Expanded Abstracts*, **26**, 323–327.